Improving the Nanoparticle Resolution of the ELPI

Jaakko Yli-Ojanperä, Jonna Kannosto, Marko Marjamäki, Jorma Keskinen[*]

Department of Physics, Tampere University of Technology, P.O. Box 692, FIN-33101 Tampere, Finland

ABSTRACT

The nanoparticle resolution of Electrical Low Pressure Impactor (ELPI) has been improved by designing and manufacturing a new impactor stage for the impactor. The measured cutpoint of the stage is 16.7 nm. The additional stage does not affect the properties (e.g. cutpoints) of other impactor stages. The performance of the new impactor construction was evaluated with laboratory and heavy duty diesel exhaust measurements. Based on the laboratory measurements the lower limit for the measured geometric mean diameter is expanded down to 11 nm. The diesel exhaust measurements made parallel with the new and the old construction show that the results are equal at large particle sizes. For nanoparticles, the resolution and precision are improved with the new construction. Using the new impactor stage and density analyzing method density can be analyzed even for 10 nm particles.

Keywords: Nanoparticle; Impactor; ELPI.

INTRODUCTION

Electrical Low Pressure Impactor (ELPI) is an instrument that can be used to measure the concentration and size distribution of particles as a function of aerodynamic particle size in real-time (Keskinen *et al.*, 1992; Marjamäki *et al.*, 2000). In ELPI's cascade impactor, the sampled and unipolarly charged aerosol is classified into size fractions. The currents resulting from the collected charged particles are measured simultaneously from electrically insulated impactor stages with electrometers. The nominal flow rate of the instrument is 10 L/min. In the original construction the particle size range measured by the ELPI is from 30 nanometers to 10 micrometers. Marjamäki *et al.* (2002) extended the electrically measured size range down to 7 nanometers by adding a filter stage last in the flow direction of the device. Even in this configuration there is no size classification for the particles below 30 nanometers.

The instrument has been widely used to various applications, such as diesel exhaust measurement (e.q. Maricq *et al.*, 2000; Gulijk *et al.*, 2003; Ntziachristos *et al.*, 2004; Ristimäki *et al.*, 2006). When diluted, the diesel exhaust aerosol frequently displays a nucleation mode (e.g. Kittelson, 1998; Giechaskiel *et al.*, 2005; Rönkkö *et al.*, 2007) that largely escapes the original lower particle size (30 nm) of the ELPI. For these applications, additional size information below 30 nanometers would be important.

Along with the Differential Mobility Analyzer (DMA; Knutson and Whitby, 1975) and the Scanning Mobility Particle Sizer (SMPS; Wang and Flagan, 1990) the ELPI has been found useful in measuring the effective density of the particles in diesel exhaust measurements (Ahlvik *et al.*, 1998; Maricq *et al.*, 2000; Ristimäki *et al.*, 2002) and in ambient air measurements (Virtanen *et al.*, 2006; Kannosto *et al.*, 2008). The density of the nanoparticles is of particular interest because it is related to the forming mechanism and physical properties of the particles. To be able to understand and predict the new particle forming and growth, it is necessary to have size resolution below 30 nanometers.

The purpose of this work was to improve the precision and the resolution power of the electrical low pressure impactor in measuring number concentrations of nanoparticles (<30 nm). For this purpose a new additional impactor stage was designed and manufactured. With the help of the new stage the particle size range normally collected by the filter stage is divided between the new stage and the filter stage. This allows improved size resolution and improves the number concentration accuracy, because the wide particle size range of the filter stage can lead to overestimation in the number concentration (Marjamäki *et al.*, 2002). In the presented configuration the classified aerodynamic particle size range is expanded from 30 nm down to 16.7 nm. These improvements in size resolution and concentration measurement will result in better accuracy for the measured effective densities of nanoparticles.

DESIGN

The new stage is designed to be installed between the filter stage and the 1st stage. In order to add the new stage to

---
[*] Corresponding author. Tel.: +358-3-3115-2676;
Fax: +358-3-3115-2600
E-mail address: jorma.keskinen@tut.fi

the impactor the stage 10 is removed from the construction. The outer dimensions and the widths of the nozzle and collection plates are chosen to be the same as in stages from 1 to 10 to avoid additional mechanical changes. The desired cutpoint is within 16–18 nm which is approximately the geometric mean diameter between the cutpoints of the filter stage (7 nm) and the 1st stage (32.4 nm). In addition to other designing criteria, the new stage must not affect in any way the operation of other impactor stages. This means two things: The absolute pressure after stage 1 should be same after adding the new stage (100 mbar) and the mass flow rate of the stage must be equal to the ELPI's flow rate. The volumetric flow rate of the particular unit is 9.73 L/min at 1013.3 mbar inlet pressure and at 20°C temperature. Within the limits set by the ELPI the stage must have the best attainable impaction properties.

The operation of an impactor stage is characterized by the collection efficiency curve. The cutpoint of the stage (D_{50}) is defined as a particle size that has 50 percent collection efficiency. The slope of the curve is calculated as a ratio of diameters corresponding to the 70% and 30% collection efficiencies (Hillamo and Kauppinen, 1991). The Stokes number corresponding to the 50 % collection efficiency (Stk_{50}) is calculated from the measured cutpoint, mass flow rate and absolute values of the upstream and the downstream stagnation pressures of the stage using a method that is clearly presented by Hillamo and Kauppinen (1991) and is based on the results of Flagan (1982), Biswas and Flagan (1984) and Hering (1987). The basic idea of the method is that the collection efficiency depends only on the particles Stokes number if the flow field of the stage is constant. While calculating the cutpoint the equation of Stokes number is presented in the following form

$$C_C D_{50}{}^2 = \frac{9 Stk_{50} W \eta}{\rho_0 V_0} \qquad (1)$$

where C_c is the slip correction factor, η is the gas viscosity, ρ_0 is the density for aerodynamic particles (1000 kg/m³), V_0 is the adiabatic jet velocity of the gas and W is the jet diameter. Using the equation 1 the cutpoint is calculated using iterative calculation.

In the design phase the lowest attainable cutpoints at a known inlet pressure was estimated theoretically for different nozzle diameters by assuming a critical isothermal velocity

(for air 343 m/s, $T = 20°C$) for the nozzles at pressure ratio (r) value 0.45 which is approximately the case for the stage 1 in the ELPI's cascade impactor. In addition, the highest Stk_{50} value of the ELPI's impactor stages (0.233) was used in the estimation. Both assumptions tend to slightly overestimate the cutpoint leaving room for cutpoint adjustments by increasing the downstream stagnation pressure of the new stage if needed. The estimated aerodynamic cutpoint for different nozzle diameters are presented in Table 1.

CALIBRATION OF THE IMPACTOR STAGES

The setup used for the calibration of impactor stages is presented in Fig. 1.

Polydisperse aerosol was generated from di-octyl sebacate (DOS, density = 0.912 g/cm³) using an evaporation-condensation generator described by Liu and Lee (1975). In our version of the generator, plain DOS (purity 97%) was used in the atomizer in order to minimize the changes in particle density caused by solvent impurities. The size distribution of aerosol was measured using scanning mobility particle sizer (SMPS) consisting of DMA (TSI model 3085) and CPC (TSI model 3025A). A certain monodisperse electrical mobility size selected from the distribution was passed through the DMA. The electrical current produced by the monodisperse particles was measured with ELPI from all impactor stages. Collection efficiency for a certain electrical mobility size was calculated as a ratio of collected current to total current entering the stage (Keskinen *et al.*, 1999).

Table 1. Calculated aerodynamic cutpoints and Reynolds numbers for different nozzle diameters. For each nozzle diameter a critical isothermal velocity (for air 343 m/s, $T = 20°C$) and pressure ratio (r) value 0.45 is used in the calculations.

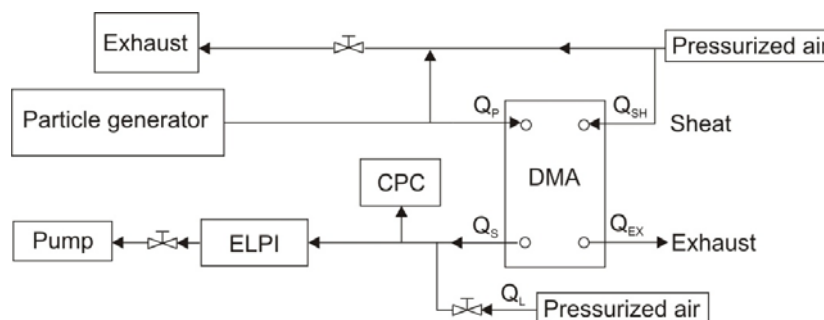| nozzle diameter W (mm)	D_{50} (nm)	Re
0.2	11.3	379
0.25	14.1	473
0.3	16.9	568
0.35	19.7	662
0.4	22.5	757
0.45	25.3	852
0.5	28.1	946

Fig. 1. Setup used for the calibration of impactor stages. DMA flow rates: $Q_p = Q_S = 1.5$ L/min, $Q_{SH} = Q_{EX} = 15$ L/min.

The measurement system was pressurized in order to adjust the impactor's inlet pressure to match the calibration conditions. In addition, the stagnation pressure between the new stage and the filter stage was used as a control pressure in order to assure the correct operation of the impactor. The flow rate of the impactor was checked before and after the measurements to avoid any error caused by the blocking of the impactor nozzles. Based to the measured (fairly narrow) size distributions (gsd 1.2–1.4) monodisperse particle sizes were selected from the right descending edge of the distributions. This was made in order to minimize the measured current resulting from multiply charged particles (Hillamo and Kauppinen, 1991).

MEASURED COLLECTION EFFICIENCY CURVE AND STAGE PARAMETERS

As mentioned earlier one of the goals in design of the new stage was that it must not affect to the operation of other impactor stages. This was verified by measuring the collection efficiencies of the stage 1 and stage 2 in two different device configurations, namely with and without the new stage installed in ELPI. Any effect of the new stage on the properties of the other stages would be seen as a change in the collection efficiency curves of stage 1 and 2. The measured collection efficiency curves are presented in Fig. 2 and they clearly show that the new stage has no effect on the collection efficiency curves of the stage 1 and 2.

The cutpoint and the steepness of the collection efficiency curve of the new stage was calculated based to the fit function made to the measurement points between collection efficiencies 0.3 and 0.7 with least squares method. These and other calculated stage properties are presented in Table 2. As Table 2 states the aerodynamic cutpoint of the new stage is in agreement with the result of

cutpoint estimation (16.9 nm) presented in Table 1. The square root of Stokes number lies within the values of the other impactor stages in ELPI (0.421–0.483, Marjamäki *et al.*, 2000) meaning that operation of stages at this low impaction pressure can be predicted with the common impactor theory. In addition, the slope of the collection efficiency curve equals to the value of stage 1. The stagnation pressure of the new stage is 43.4 mbar which means that in order to use it higher pumping capacity is needed.

The response functions of the ELPI stages for a known particle density can be calculated based to the fit functions for the collection efficiency curves made by Marjamäki *et al.* (2005). The fit functions take into account the fine particle deposition onto the stage due to diffusion and image charge which are referred as loss mechanisms. In order to characterize the response of the new device configuration the fit function for the new stage was defined following the convention used by Marjamäki *et al.* (2005). The parameters used for primary efficiency are 16.677 nm for aerodynamic cutpoint and 3.8193 for steepness of the collection efficiency curve. For diffusion and image charge collection efficiencies the parameters are 2.44 for effective stage length (L(m)) and 5.00 for image charge deposition intensity.

TESTS

Size Distribution

Fig. 3 shows the size distributions measured simultaneously with two SMPS systems and the new and the old ELPI constructions from Euro IV compliant medium duty diesel engine exhaust (model year 2006, displacement 4.5 dm^3, common-rail fuel injection, max. power 118 kW@ 2500 1/min, max. torque 600 Nm @ 1500 1/min). The particle sampling system was similar to the one
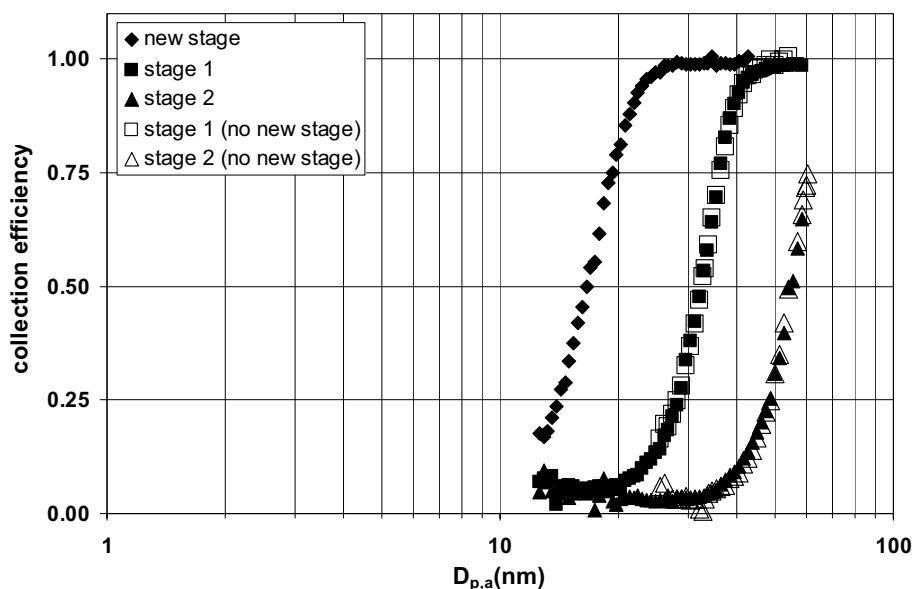

Fig. 2. The measured collection efficiency curves for two device configurations. The text "no new stage" in the parenthesis refers to the measurements where the new stage was not installed.

Table 2. Aerodynamic cutpoints and other properties of the ELPI impactor. The flow rate of the impactor is 9.73 L/min.

stage	D_{50} (μm)	Stage absolute pressure (mbar)	$\sqrt{Stk_{50}}$	slope of the collection efficiency curve	Re	V_0(m/s)
filter	0.007	–	–	–	–	–
new	0.0167	43.4	0.460	1.27	524	270
1	0.0324	100.0	0.421	1.27	1250	285
2	0.055	220.3	0.453	1.22	1490	239
3	0.094	393.3	0.439	1.31	3490	260
4	0.157	684.7	0.448	1.27	2970	173
5	0.265	892.2	0.477	1.26	1770	96
6	0.386	972.3	0.456	1.09	900	48
7	0.619	996.6	0.45	1.13	700	27.6
8	0.956	1005.5	0.445	1.09	950	21.4
9	1.61	1010.3	0.461	1.19	780	12.3
10	2.41	1011.9	0.451	1.12	680	7.6
11	4.03	1012.5	0.465	1.15	1380	6.8
12	6.74	1013.0	0.483	1.17	2110	5.3
13	9.99	1013,2	0.472	1.25	1600	3
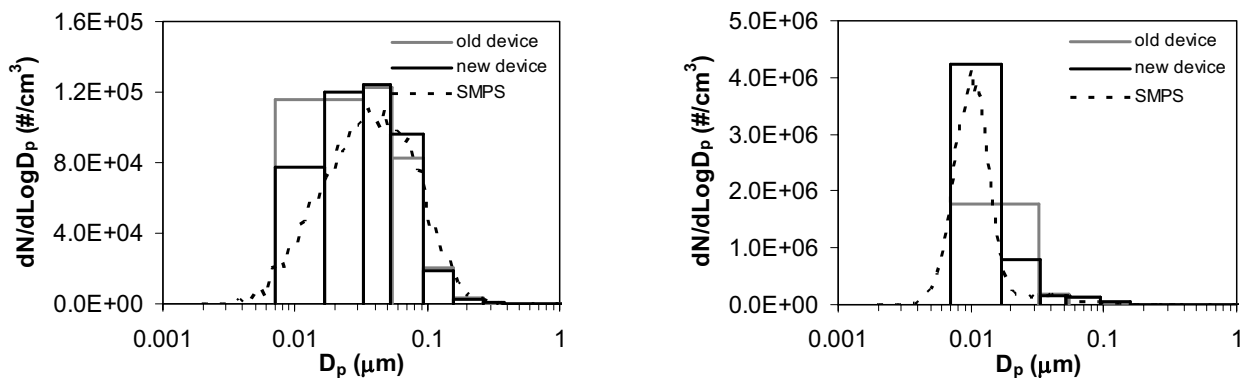
Fig. 3. Examples of the size distributions measured with different devices from Euro IV compliant medium duty diesel engine exhaust. The engine was tested in different points of European Stationary Cycle (ESC). Results from ESC11 (left) and ESC10 (right) are shown in the figure.

used by Vaaraslahti *et al.* (2004). The SMPS systems consisted of long and short DMAs (TSI models 3071, 3085) and CPCs (TSI model 3025A). The engine was tested in different points of European Stationary Cycle (ESC). In figure the size distributions are presented as a function of electrical mobility size. For the ELPI constructions we used unit density assumption in calculating the particle size distributions. From the Fig. 3 it can be seen that the results for stages outside the particle size range collected by the old filter stage have small differences for old and new device configurations. The small differences between the devices derive from the slightly different cutpoints of the cascade impactor used in the old device configuration compared to the one used simultaneously in the new one. In the size range of the old filter stage the improvement of the size resolution obtained with the new device is obvious.

The response of the new device to the changes in the geometric mean diameter of the size distribution was evaluated by generating narrow size distributions (GSD ≈ 1.2) from DOS at different geometric mean diameter values

and measuring the distributions parallel with the new device and the SMPS. The results are shown in Fig. 4.

Fig. 4(a) shows the calculated number based geometric mean diameters and the attainable theoretical lower limits for the new and the old device. From the results it can be seen that the measurable range for the geometric mean diameter is expanded down to the theoretical limit of the new device which is approximately 11 nanometers (i.e. lowest size bin geometric midpoint). The values measured with the new ELPI are somewhat smaller than the ones measured with the SMPS. This difference does not indicate the poor performance of the new impactor but it results from the limited size resolution and the change from one moment to another, namely from the measured current distribution to the number distribution.

Fig. 4(b) shows the calculated geometric mean diameters weighted by the current carried by the charged particles. This shows the performance of the impactor alone and the results for the new device and the SMPS are close to the ideal one to one response.
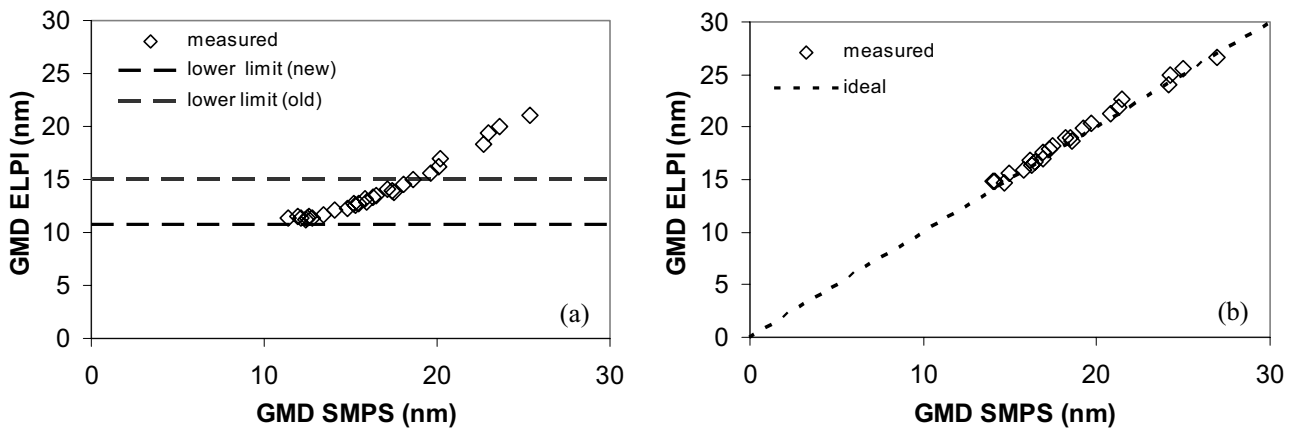
Fig. 4. Geometric mean diameters weighted by the number concentration (a) and the current carried by the particles (b) calculated from the results measured parallel with the new device and the SMPS. The current size distributions for the SMPS are calculated by multiplying the measured particle distribution with the charging efficiency of the ELPI's charger. The current size distributions of the ELPI are direct measurement results.

Particle Density

The density response of the method presented by Ristimäki *et al.* (2002) was tested with simulations and measurements. The simulations were made for the new and the old device configurations for single mode lognormal size distributions. The used geometric standard deviation of the size distributions was 1.2 and the simulations were made for the following geometric mean diameters: from 6 to 20 nm at 1 nm steps and from 25 to 40 nm at 5 nm steps. The density values of the initial particle modes were 1.0 g/cm³. In order to estimate the sensitivity of the particle density calculation to measurement errors of ELPI a similar method as presented by Virtanen *et al.* (2004) was used. In our case a five percent random noise was added to the simulated ELPI stage currents. For each size distribution the density calculation was made 50 times.

Fig. 5 shows the standard deviation (STD) of each 50 calculation set, both for the old and new device configuration. The simulation runs produced densities agreeing with the input density for both device configurations for GMD values higher than 20 nm. Below that, the density values for the old configuration started to scatter for each input distribution, shown as a rapid increase in the STD for lower GMD values. The new device configuration works well down to approximately 10 nm GMD. Allowing some deviation in density values the lowest measurable GMD values can be estimated to be 20 nm and 10 nm for the old and new device configurations, respectively. These limits are in aerodynamic diameters and they are affected by particle's density: higher GMD would be required for particles with density lower than 1.0 g/cm³, while lower GMD distributions could be measured for particles with density exceeding 1.0 g/cm³.

Laboratory tests of the density analyzing method were taken using DOS and evaporation-condensation generator to produce polydisperse aerosol distribution. The geometric mean diameter of the particles size distribution varied between 8 nm–40 nm and the distributions were rather narrow, with geometric standard deviation of 1.2–

1.4. The mobility size distribution was measured with the SMPS while the aerodynamic size of particles was measured using ELPI with the new impactor stage.

In the measurements, only the new device configuration was used. Current values for the old configuration were calculated by summing up currents of the filter stage and the new stage from the new configuration. Density results calculated for both configurations are shown in Fig. 6. The density values obtained for the DOS particle distributions are close to the bulk density value of DOS for GMD values higher than 15 nm. The first density values deviating more than 20% from the bulk value are obtained for approximately 13 nm for the old configuration and 8 nm for the new configuration.

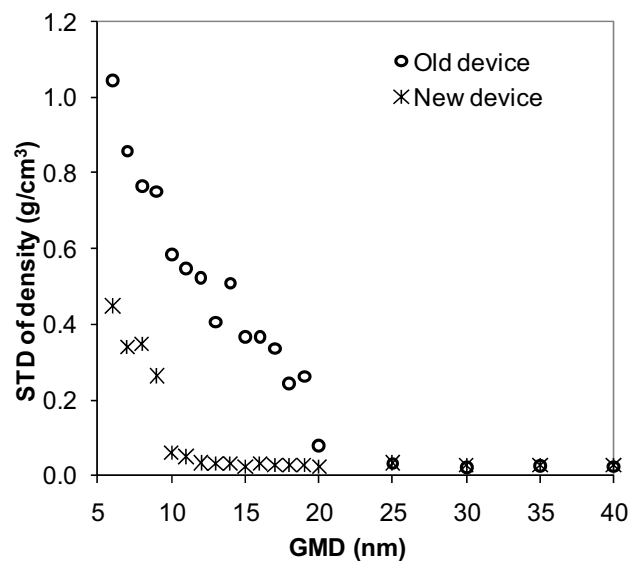Figs. 5 and 6 indicate that with the help of the new

Fig. 5. The result of the simulation. STD of density results increases as mode GMD decreases. The Deviation of the old (open circles) and the new impactor device (black stars) start to increase after 20 nm and 10 nm, respectively.
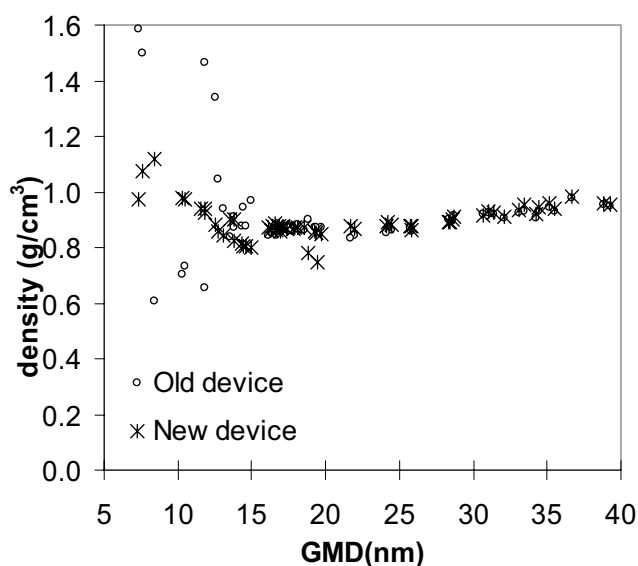
Fig. 6. The measured density values of DOS as a function of mode GMD (mobility). The stars are measured using the new impactor setup and open circles are results of the old impactor setup.

device it is possible to measure the density of nanoparticles to smaller particle sizes than with the old device. Both simulation and the test measurement indicate that with the new device configuration it is possible to measure particle density for polydispersed aerosol with a GMD value as low as 10 nm. However, this provides that the instruments are carefully calibrated and that the particles do not bounce.

CONCLUSIONS

A new impactor stage was designed and manufactured to improve the precision and the resolution power of the electrical low pressure impactor in measuring number concentrations of nanoparticles. The cutpoint of the new stage is 16.7 nm which is practically the same as the theoretically estimated value 16.9 nm. The installation of the new stage as a part of ELPI's cascade impactor does not affect the operation of the other impactor stages. This means that the cutpoints of the other stages remain the same and the results measured with the new and the old impactor constructions are comparable.

The new stage can be mounted to other impactor units with the same dimensioning used in this work, if less than 4 percent changes are allowable in the cutpoints of the new stage and stages one and two. Otherwise the dimensioning should be made separately for each impactor unit. The only drawback in mounting of the new stage is the nearly threefold need for pump capacity because of a reduced outlet pressure of the impactor.

Based on the test measurements made parallel for the new and the old constructions, the resolution improved with the new construction compared to the old construction in the particle size range collected by the old filter stage (7–32.4 nm). Along with the new construction the lower limit for the measured geometric mean diameter

is expanded down to the theoretical limit of the new construction, which is approximately 11 nanometers.

The performance of the method used in calculating the effective density of the nanoparticles is improved and the density of particles down to 10 nm can be measured with relatively small error. In overall the new device construction should be better suited for measuring nanoparticles than the old one. In our upcoming work, we will study the effects of the new stage on the data inversion methods, such as presented by Lemmetty *et al.* (2005).

ACKNOWLEDGEMENTS

REFERENCES

Ahlvik, P., Ntziachristos, L., Keskinen, J. and Virtanen, A. (1998). Real Time Measurements of Diesel Particle Size Distributions with an Electrical Low Pressure Impactor. *SAE Technical Paper Series* 980410.

Biswas, P. and Flagan, R.C. (1984). High-Velocity Inertial Impactors. *Environ. Sci. Technol.* 18: 611–616.

Flagan, R.C. (1982) Compressible Flow Inertial Impactors. *J. Colloid Interface Sci.* 87: 291–299.

Giechaskiel, B., Ntziachristos, L., Samaras, Z., Scheer, V., Casati, R. and Vogt, R. (2005) Formation Potential of Vehicle Exhaust Nucleation Mode Particles On-road and in the Laboratory. *Atmos. Environ.* 39: 3191–3198.

Gulijk, C., Marijnissen, J.C.M., Makkee, M. and Moulijn, J.A. (2003). Oil-soaked Sintered Impactors for the ELPI in Diesel Particulate Measurements. *J. Aerosol Sci.* 34: 635–640.

Hering, S.V. (1987). Calibration of the QCM Impactor for Stratospheric Sampling. *Aerosol Sci. Technol.* 7: 257–274.

Hillamo, R.E. and Kauppinen, E.I. (1991). On the Performance of the Berner Low Pressure Impactor. *Aerosol Sci. Technol.* 14: 33–47.

Kannosto, J., Lemmetty, M., Virtanen, A., Mäkelä, J.M., Keskinen, J., Junninen, H., Hussein, T., Aalto, P. and Kulmala, M. (2008). Mode Resolved Density of Atmospheric Aerosol Particles. *Atmos. Chem. Phys.* 8: 5327–5337.

Keskinen, J., Marjamäki, M., Virtanen, A., Mäkelä, T. and Hillamo, R. (1999). Electrical Calibration Method for Cascade Impactors. *J. Aerosol Sci.* 30: 111–116.

Keskinen, J., Pietarinen, K. and Lehtimäki, M. (1992). Electrical Low Pressure Impactor. *J. Aerosol Sci.* 23: 353–360.

Kittelson, D. (1998). Engines and Nanoparticles: A Review. *J. Aerosol Sci.* 29: 575–588.

Knutson, E.O. and Whitby, K.T. (1975). Aerosol Classification by Electric Mobility: Apparatus, Theory and Applications. *J. Aerosol Sci.* 6: 443–451.

Lemmetty, M., Marjamäki, M. and Keskinen J. (2005). The ELPI Response and Data Reduction II: Properties

of Kernels and Data Inversion. *Aerosol Sci. Technol.* 39: 583–595.

Liu, B.Y.H. and Lee, K.W. (1975). An Aerosol Generator of High Stability. *Am. Ind. Hyg. Assoc. J.* 36:861–865.

Maricq, M.M., Podsiadlik, D.H., and Chase, R.E. (2000). Size Distributions of Motor Vehicle Exhaust PM: A Comparison between ELPI and SMPS Measurements. *Aerosol Sci. Technol.* 33: 239–260.

Marjamäki, M., Keskinen, J., Chen, Da-Ren and Pui, D.Y.H. (2000). Performance Evaluation of the Electrical Low-pressure Impactor (ELPI). *J. Aerosol Sci.* 31: 249–261.

Marjamäki, M., Lemmetty, M. and Keskinen, J. (2005). ELPI Response and Data Reduction I: Response Functions. *Aerosol Sci. Technol.* 39: 575–582.

Marjamäki, M., Ntziachristos, L., Virtanen, A., Ristimäki, J., Keskinen, J., Moisio, M., Palonen, M. and Lappi, M. (2002). Electrical Filter Stage for the ELPI. *SAE Technical Paper Series* 2002-01-0055.

Moisio, M. (1999). Real Time Size Distribution Measurement of Combustion Aerosols. PhD. Thesis. Tampere University of Technology.

Ntziachristos, L., Giechaskiel, B., Pistikopoulos, P., Samaras, Z., Mathis, U., Mohr, M., Ristimäki, J., Keskinen, J., Mikkanen, P., Casati, R., Scheer and Vogt, R. (2004). Performance Evaluation of a Novel Sampling and Measurement System for Exhaust Particle Characterization. *SAE Technical Paper Series* 2004-01-1439.

Ristimäki, J., Vaaraslahti, K., Lappi, M. and Keskinen, J. (2006). Hydrocarbon Condensation in Heavy-Duty Diesel Exhaust. *Environ. Sci. Technol.* 41: 6397–6402.

Ristimäki, J., Virtanen, A., Marjamäki, M., Rostedt, A. and Keskinen, J. (2002). On-line Measurement of Size Distribution and Effective Density of Submicron Aerosol Particles. *J. Aerosol Sci.* 33: 1541–1557.

Rönkkö, T., Virtanen, A., Kannosto, J., Keskinen, J., Lappi, M. and Pirjola, L. (2007). Nucleation Mode Particles with a Nonvolatile Core in the Exhaust of a Heavy Duty Diesel Vehicle. *Environ. Sci. Technol.* 41: 6384–6389.

Vaaraslahti, K., Virtanen, A, Ristimäki, J. and Keskinen, J. (2004). Nucleation Mode Formation in Heavy-duty Diesel Exhaust with and without a Particulate Filter. *Environ. Sci. Technol.* 38: 4884–4890.

Virtanen, A., Ristimäki, J. and Keskinen, J. (2004). New Method to Define the Effective Density and Fractal Dimension of Agglomerate Particles. *Aerosol Sci. Technol.* 38: 437–446.

Virtanen, A., Rönkkö, T., Kannosto, J., Mäkelä, J.M., Keskinen, J., Pakkanen, T., Hillamo, R., Pirjola, L. and Hämeri, K. (2006). Winter and Summer Time Size Distribution and Densities of Traffic Related Aerosol Particles at a Busy Highway in Helsinki. *Atmos. Chem. Phys.* 6: 2411–2421.

Wang., S.C. and Flagan, R.C. (1990). Scanning Electrical Mobility Spectrometer. *Aerosol Sci. Technol.* 13: 230–240.